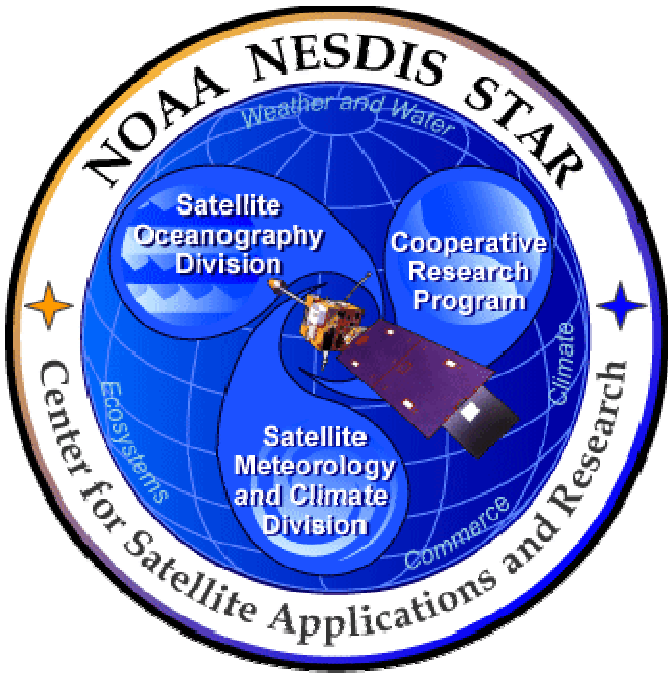


**NOAA NESDIS**
**CENTER for SATELLITE APPLICATIONS**
**and RESEARCH**

# GOES-R Advanced Baseline Imager (ABI) Algorithm Theoretical Basis Document For Green Vegetation Fraction

*Peter Romanov, University of Maryland*
*Yuhong Tian, I and M System Group, Inc.*
*Yunyue Yu, NOAA/NESDIS/STAR*
*Dan Tarpley, Short & Associates, Inc.*

Version 1.0
September 15, 2010

GOES-R ABI GVF ALGORITHM THEORETICAL BASIS DOCUMENT
VERSION HISTORY SUMMARY

| Version | Description | Revised Sections | Date |
|---|---|---|---|
| 0.0 | New ATBD Document according to NOAA /NESDIS/STAR Document Guideline | | 09/21/2008 |
| 0.1 | New ATBD Document according to NOAA /NESDIS/STAR Document Guideline | | 09/30/2008 |
| 1.0 | ATBD Document with 80% readiness of algorithm development software improvement | | 06/30/2010 |

**TABLE OF CONTENTS**

Page

## LIST OF FIGURES

Page

## LIST OF TABLES

Page

## LIST OF ACRONYMS

| | |
|---|---|
| ABI | Advanced Baseline Imager |
| AIT | Algorithm Integration Team |
| ATBD | Algorithm Theoretical Basis Document |
| AWG | Algorithm Working Group |
| CDR | Critical Design Review |
| CICS | Cooperative Institute for Climate Studies |
| CIMSS | Cooperative Institute for Meteorological Satellite Studies |
| CM | Configuration Management |
| DG | Document Guideline |
| EPL | Enterprise Product Lifecycle |
| GS-F&PS | Ground Segment Functional and Performance Specification |
| GVF | Green Vegetation Fraction |
| IMS | Interactive Multi-sensor snow and ice mapping System |
| MSG | Meteosat Second Generation |
| NDVI | Normalized Difference Vegetation Index |
| NESDIS | National Environmental Satellite, Data, and Information Service |
| NIR | Near InfraRed |
| NOAA | National Oceanic and Atmospheric Administration |
| OCD | Operations Concept Document |
| OSDPD | Office of Satellite Data Processing and Distribution |
| QA | Quality Assurance |
| QC | Quality Control |
| SEVIRI | Spinning Enhanced Visible and Infra-red Imager |
| SSEC | Space Science and Engineering Center |
| STAR | Center for Satellite Applications and Research |
| TOA | Top of Atmosphere |
| TOC | Top of Canopy |
| VIS | VISible Channel |
| VVP | Verification and Validation Plan |

# ABSTRACT

Green Vegetation Fraction (GVF) is the fraction of area within the instrument footprint occupied by green vegetation. The Numerical Weather Prediction (NWP) and climate models need this parameter to partition the fraction of the surface in the model grid cell that is evaporating and transpiring at rates controlled by vegetation as opposed to the fraction of the surface evaporating as bare soil surface. The algorithm to derive GVF from observations of the Advanced Baseline Imager (ABI) instrument onboard GOES-R satellite is based on the Normalized Difference Vegetation Index (NDVI). An NDVI-based linear mixture approach has been chosen to convert NDVI into GVF. A similar technique has been historically used at NOAA/NESDIS to generate GVF from observations of Advanced Very High Resolution Radiometer (AVHRR) onboard NOAA satellites. The GVF algorithm has been developed and tested using observations from the SEVIRI sensor onboard the European Meteosat Second Generation (MSG) geostationary satellite. Studies of SEVIRI data have shown that NDVI strongly depends upon the viewing and illumination geometry of observations, especially over dense vegetation. If not corrected, this angular anisotropy of NDVI causes substantial spurious diurnal variations in the derived GVF. An empirical kernel-driven model to correct NDVI for angular anisotropy has been developed and implemented in the GVF algorithm. Its kernel weights as well as endmember values for the GVF algorithm were also determined empirically from SEVIRI clear-sky data. The preliminary validation estimates show that the algorithm meets performance requirements. The current document describes the algorithm that will be used to derive GVF from instantaneous GOES-R ABI imagery. As it is required by the Ground Segment Functional and Performance Specification (GS-F & PS) the GVF product will be generated on an hourly basis. In the future in addition to the standard hourly GVF product, tailored products such as daily and weekly composited maps of GVF will be developed.

# 1 INTRODUCTION

## 1.1 Purpose of This Document

The GOES-R ABI GVF algorithm theoretical basis document (ATBD) provides a high level description of the theoretical basis for the derivation of the GOES-R Green Vegetation Fraction (GVF) products using observations from the Advanced Baseline Imager (ABI) flown on the GOES-R series of NOAA geostationary meteorological satellites. GOES-R ABI will be the first GOES imaging instrument providing observations in both the visible and the near infrared spectral bands which can be used to generate Normalized Difference Vegetation Index (NDVI) values for monitoring the state of the vegetation cover as well as identifying areas of vegetation stress and drought. The GVF is derived from the ABI NDVI product.

## 1.2 Who Should Use This Document

The intended users of this document are those interested in understanding the physical basis of the GVF algorithm and how to use the output of the algorithm to optimize the GVF for a particular application. This document also provides information useful to anyone maintaining or modifying the original algorithm.

## 1.3 Inside Each Section

This document has the the following main sections.

- **System Overview**: Provides relevant details of the ABI and provides a brief description of the products generated by the algorithm.

- **Algorithm Description**: Provides all the detailed description of the algorithm including the physical basis, input and output.

- **Assumptions and Limitations**: Provides an overview of the current limitations of the approach and the plan for overcoming these limitations with further algorithm development.

## 1.4 Related Documents

This document currently does not relate to any other document other than the GOES-R Ground Segment Functional and Performance Specification (GS-F&PS).

## 1.5 Revision History

Version 0.0 of this document was created to accompany the delivery of the version 0.0 algorithm to the GOES-R AWG Algorithm Integration Team (AIT). It was then modified to be as version 0.1.

Version 1.0 of this document was created upon modification of the draft ATBD to reflect changes/improvement made for the 80% readiness document, including some additions/changes conducted from the algorithm Critical Design Review (CDR).

# 2 OBSERVING SYSTEM OVERVIEW

This section describes the products generated by the ABI GVF algorithm and the related sensor requirements.

## 2.1 Products Generated

Green vegetation fraction (GVF) is one of land surface products that will be routinely generated by the GOES-R data processing system. GVF will be generated from GOES-R ABI data and presents the fraction of green vegetation within the instrument footprint. Information on the green vegetation fraction is needed in land surface models where it is used to partition the fraction of the surface in the model grid cell into evapotranspiration controlled by vegetation and into evaporation controlled by bare soil (Ek et al, 2003; Barlage and Zeng, 2004).

Green vegetation fraction will be derived from another GOES-R ABI operational product, the Normalized Difference Vegetation Index (NDVI). The GVF product will be generated in day-time clear sky conditions for the GOES-R full disk area and will be delivered on an hourly basis. The GVF product will satisfy requirements presented in the GOES-R Ground Segment Functional and Performance Specification (GS-F & PS) in table 2.1.

*Table 2.1. Functional & Performance Specification (GS-F&PS) for ABI GVF*

| Name | User & Priority | Geographic Coverage (G, H, C, M) | Vertical Res. | Horiz. Res. | Mapping Accuracy | Msmnt. Range | Msmnt. Accuracy | Refresh Rate/Coverage Time Option (Mode 3) | Refresh Rate Option (Mode 4) | Data Latency | Product Measurement Precision | Long-Term Stability | Temporal Coverage Qualifiers | Product Extent Qualifier | Cloud Cover Conditions Qualifier | Product Statistics Qualifier |
|---|---|---|---|---|---|---|---|---|---|---|---|---|---|---|---|---|
| Vegetation Fraction: Green | GOES-R | Full Disk | N/A | 2 km | 1 km | 0 to 1 (unitless) | 0.10 for LZA below 55; 0.20 for LZA 55~70 degrees | 60 min | 60 min | 3236 sec | 0.10 for LZA below 55; 0.20 for LZA 55~70 degrees | TBD | Sun at 67 degree solar zenith angle | Quantitative out to at least 70 degrees LZA and qualitative beyond | Clear Conditions associated with threshold accuracy | Over specified geographic area |

[1] LZA=local zenith angle

## 2.2 Instrument Characteristics

GOES-R ABI radiometer will provide routine observations of the Earth in 16 spectral channels located in the visible, near infrared, shortwave infrared and thermal infrared spectral range. The GVF product will be derived from the ABI NDVI product. No additional ABI sensor data other than involved in the NDVI algorithm will be used to generate the GVF product. GVF values will

be estimated for each pixel observed by the ABI where valid NDVI retrieval is available. Table 2.2 identifies the ABI channels and shadows those used for the NDVI algorithm

*Table 2.2. Spectral characters of Advanced Baseline Imager*

| Channel Number | Wavelength (μm) | Bandwidth (μm) | NEDT/SNR | Upper Limit Of Dynamic Range | Spatial Resolution |
|---|---|---|---|---|---|
| 1 | 0.47 | 0.45 – 0.49 | 300:1[1] | 652 $W/m^2/sr/\mu m$ | 1 km |
| 2 | 0.64 | 0.59 – 0.69 | 300:1[1] | 515 $W/m^2/sr/\mu m$ | 0.5 km |
| 3 | 0.86 | 0.8455 – 0.8845 | 300:1[1] | 305 $W/m^2/sr/\mu m$ | 1 km |
| 4 | 1.38 | 1.3705 – 1.3855 | 300:1[1] | 114 $W/m^2/sr/\mu m$ | 2 km |
| 5 | 1.61 | 1.58 – 1.64 | 300:1[1] | 77 $W/m^2/sr/\mu m$ | 1 km |
| 6 | 2.26 | 2.225 – 2.275 | 300:1[1] | 24 $W/m^2/sr/\mu m$ | 2 km |
| 7 | 3.9 | 3.8 – 4.0 | 0.1K[2] | 400K | 2 km |
| 8 | 6.15 | 5.77 – 6.60 | 0.1K[2] | 300K | 2 km |
| 9 | 7.0 | 6.75 – 7.15 | 0.1K[2] | 300K | 2 km |
| 10 | 7.4 | 7.24 – 7.44 | 0.1K[2] | 320K | 2 km |
| 11 | 8.5 | 8.30 – 8.70 | 0.1K[2] | 330K | 2 km |
| 12 | 9.7 | 9.42 – 9.80 | 0.1K[2] | 300K | 2 km |
| 13 | 10.35 | 10.10 – 10.60 | 0.1K[2] | 330K | 2 km |
| 14 | 11.2 | 10.80 – 11.60 | 0.1K[2] | 330K | 2 km |
| 15 | 12.3 | 11.80 – 12.80 | 0.1K[2] | 330K | 2 km |
| 16 | 13.3 | 13.0 – 13.6 | 0.3K[2] | 305K | 2 km |

[1]100% albedo, [2]300K scene. Shaded channels are used for NDVI calculation.

## 2.3 Mission Requirement

The GVF will be produced according to requirements formulated in the GOES-R Ground Segment Functional and Performance Specification (GS-F & PS) document listed in table 2.1. GVF will be derived over CONUS area at 60 minutes interval. The horizontal resolution is 2 km. The temporal coverage is for daytime with solar zenith angle within 67 degree. The retrieval is over land pixel with cloud clear condition. The product accuracy and precision requirement is 0.10 GVF units for satellite zenith angles below 55 deg and at 0.20 GVF units for satellite zenith angles within 55 to 70 degrees.

## 2.4 Retrieval Strategies

To derive the Green Vegetation Fraction the ABI NDVI product is used. GVF is estimated with a linear unmixing algorithm with two end-members representing fully vegetated land and bare ground surface. It is important that GOES-R ABI NDVI is the top of the atmosphere NDVI. It is derived directly from satellite-observed directional reflectances in the visible and near infrared spectral bands which are not corrected for atmospheric effects. As a result the derived NDVI is

dependent not only on the reflective properties of the land surface, but also on the particular viewing and illumination geometry of observations.

Within the GVF algorithm NDVI is corrected for angular anisotropy with a empirical kernel-driven model. End-member NDVI values as well as kernel weights in the NDVI angular anisotropy model are determined empirically from satellite observations. GVF estimates are not performed over water surface, cloudy pixels, pixels with insufficient solar illumination and any other pixels were NDVI estimates are not available for any reason. The quality of GVF retrieval is characterized by a set of quality flags provided with the product. Quality flags are assigned to each pixel.

# 3 ALGORITHM DESCRIPTION

This section presents a complete description of the algorithm at the current level of maturity (which is expected to improve with each revision).

## 3.1 Algorithm Overview

Green vegetation fraction is defined as fraction of the area within the instrument footprint occupied by green vegetation. In land models GVF is used to partition direct (bare soil) evaporation from canopy transpiration. GVF values range from 1.0 for a completely closed vegetation canopy to 0.0 for non-vegetated surfaces such as a desert or bare ground. To satisfy GOES-R Ground Segment Functional and Performance Specification (GS-F&PS), ABI-based GVF products will be derived over the full disk at a refresh rate of 60 minutes. GS-F&PS document requires the product accuracy and precision to be at 0.10 GVF units for satellite zenith angles below 55 deg and at 0.20 GVF units for satellite zenith angles within 55 to 70 degrees. The details of the GS-F&PS performance specifications are given in Table 3.1 below.

GVF is one of the option-2 products in the GOES-R ABI processing system. It relies on the high quality cloud mask to determine pixels that can be used in clear-sky retrievals of land surface properties. It also uses snow cover mask to delineate areas where vegetation cover is affected by snow. GVF retrievals require daylight conditions: No estimates are made for solar zenith angle above 67 degree.

The GVF algorithm for GOES-R ABI generally follows the traditional approach to GVF retrieval presented, in particular in Gutman and Ignatov (1998) and in Jiang, et al (2010). Within this approach the observed NDVI characterizes the state of vegetation within the pixel. GVF is derived with a linear mixture technique where end-members are global NDVI values corresponding to completely vegetated and to completely non-vegetated land surface ($NDVI_{max}$ and $NDVI_{min}$, respectively):

$$GVF = \frac{NDVI - NDVI_{\min}}{NDVI_{\max} - NDVI_{\min}} \tag{3.1}$$

Since ABI NDVI is derived from directional reflectances observed at the top of the atmosphere, NDVI changes with changing viewing and illumination geometry. In the algorithm all NDVI values are corrected for the angular anisotropy and are brought to a reference viewing-illumination geometry of observation. This is done to ensure consistency of GVF retrievals both in space and time. Minimum and maximum values of NDVI as well as parameters of NDVI angular anisotropy model are determined empirically from satellite observations.

## 3.2 Processing Outline

The processing outline of the GVF is summarized in Figure 3.1. To run the algorithm datasets of the following three categories are acquired: (1) satellite data which include angle values and level 1b Quality Control (QC) flags, (2) model data including estimated global minimum and maximum values of NDVI along with the NDVI angular anisotropy model parameters and (3) ancillary data which include ABI NDVI retrievals and NDVI QC flags. A detailed description of input datasets is provided in the following sections of the document

The GOES-R ABI GVF product is derived for all pixels where valid NDVI retrievals are available. To derive GVF all observed NDVI values along with $NDVI_{min}$ and $NDVI_{max}$ are first brought to a reference viewing-illumination geometry of observations. At the next stage a linear-mixture algorithm is applied to estimate GVF from the angular corrected NDVI. The derived GVF values along with GVF quality control flags are saved in corresponding output files.

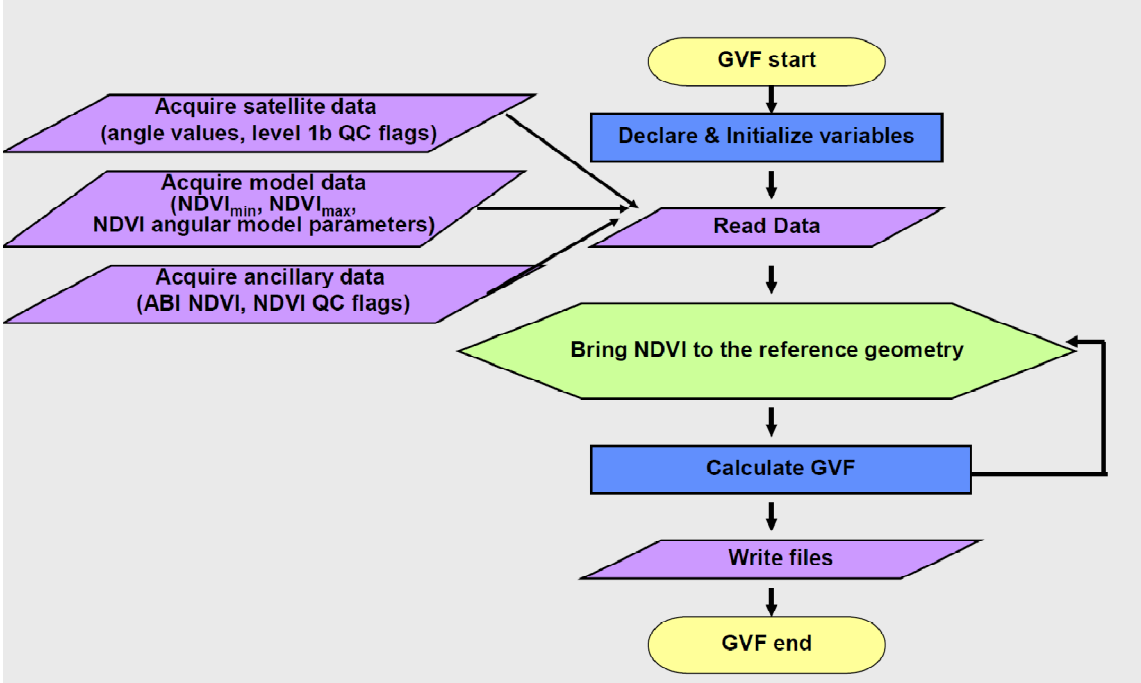


Figure 3.1. Flowchart of Green Vegetation Fraction products.

## 3.3 Algorithm Input

This section describes the input needed to process the GVF.

### 3.3.1 Primary Sensor Data

The list below contains the primary sensor data used by the GVF retrieval. By primary sensor data, we mean information that is derived solely from the ABI observations and geolocation information, or the level 1b data. Table 3.1 lists those input sensor data and their descriptions.

The GVF product is based on other GOES-R ABI products (NDVI, cloud mask, snow cover) and does not directly use information from any ABI spectral channels. However it uses information on the geometry of ABI observations including solar zenith, solar azimuth, satellite zenith and satellite azimuth angles. Information on these angles is needed to perform anisotropical correction of NDVI for GVF retrievals.

*Table 3.1. Input list of primary sensor data.*

| Name | Type | Description | Dimension |
|---|---|---|---|
| Solar zenith | input | ABI solar zenith angles | grid (xsize, ysize) |
| Solar azimuth* | input | ABI solar azimuth angles | grid (xsize, ysize) |
| View zenith | input | ABI view zenith angle | grid (xsize, ysize) |
| View azimuth* | input | ABI view azimuth angle | grid (xsize, ysize) |
| QC flags | input | ABI quality control flags with level 1b data | grid (xsize, ysize) |

*In the GVF algorithm, the relative azimuth (i.e. difference of the two azimuth values) is used.

### 3.3.2 Derived Sensor Data (GOES-R Product Precedence Data)

A number of previously computed GOES-R products are required as input data to run the GVF algorithm. The primary input to the GVF algorithm is the ABI NDVI product. There are two ABI derived sensor data sets used in the NDVI retrieval: 1) the ABI cloud mask (ACM) product, which characterizes cloudiness conditions for each pixel as clear, probably clear, probably cloudy, or cloudy, and 2) the snow mask which indicates whether the pixel is affected by snow. The fractional snow cover (FSC) is an ABI level-2 product reporting the fraction of snow in each ABI pixel and available at a refresh rate of 60 minutes.

Information on the cloud cover and snow is contained in Quality Control flags provided for the NDVI product. Therefore only NDVI product is utilized by the GVF algorithm. Table 3.2 describes the derived sensor data needed for GVF generation.

*Table 3.2. Input list of derived sensor data.*

| Name | Type | Description | Dimension |
|---|---|---|---|
| NDVI | input | ABI NDVI product calculated from calibrated ABI level 1b TOA reflectance in channels 2 and 3 | grid (xsize, ysize) |
| NDVI QC flages | input | ABI NDVI quality control flags | grid (xsize, ysize) |

### 3.3.3 Ancillary Data

Ancillary data are the non-GOES-R data that provide information not included in the primary sensor data or the previously computed GOES-R data. The only ancillary information the GVF algorithms needs is the land/water mask. This information will be acquired from Quality Control flags supplied with the NDVI product.

### 3.3.4 Algorithm Coefficients and Control values

In addition to the sensor data and the ancillary data, algorithm coefficients are ingested as the input data. Table 3.3 lists the algorithm coefficients for GOES-R ABI GVF algorithm.

*Table 3.3. Input of algorithm coefficients for GOES-R ABI GVF*

| Name | Type | Description | Dimension |
|---|---|---|---|
| Kernel Weights | input | Algorithm NDVI angular anisotropy model coefficients | 3 coefficients |
| NDVI Coefficients | input | Global NDVI maximum and minimum values $NDVI_{max}$ and $NDVI_{min}$ | 2 values |
| Reference Angle Coefficients | input | Reference geometry information | 3 values |

## 3.4 Theoretical Description

The GVF is defined as the fraction of the area within the instrument footprint occupied by green vegetation. Information on green vegetation fraction is needed when estimating the surface energy balance in numerical weather prediction (NWP) and climate models. Global and regional NWP models of the National Center for Environmental Prediction (NCEP) use GVF information to partition the model grid cell into evapotranspiration surface controlled by vegetation and into evaporation surface controlled by bare soil. In addition, GVF is a sensitive indicator of land use, land degradation, and desertification.

### 3.4.1 Physics of the Problem

Realistic characterizations of vegetation type, amount and cover and their dynamics (e.g., seasonal and inter-annual) are of great importance in describing land surface processes in weather and climate models. Green vegetation fraction (GVF) and fractional vegetation cover (FVC) are two mostly used parameters to describe the fractional presence of vegetation through growing seasons over land surface, depending on how the vegetation fraction is treated in model parameterizations. Some land surface models (e.g., NCAR Community Land Model) utilize an annual constant FVC value with a varying leaf area index (LAI) throughout the growing season

(Zeng et al., 2000), while NCEP operational forecast models use a varying GVF but a prescribed constant LAI value in their land surface model components (e.g. Noah land surface model) (Mitchell et al., 2001, Ek et. al. 2003).

GVF is different from FVC. The former is a description of how "green" a land pixel is seen from space. The latter just tells the fraction of the pixel that is occupied by vegetation, regardless whether such vegetation is green (e.g., full growth) or not green (e.g., partial growth or dormant), while the underlying assumption is that the "greenness" part is reflected by another parameter, LAI (Jiang et al., 2010). FVC is not directly linked to the real-time satellite-observed surface greenness (e.g., NDVI), as it is a constant quantity as seasons change within an annual cycle.

Generally, there are two approaches to derive vegetation fraction from satellite observations. One is multispectral mixture approaches (DeFries et al., 1999; Hansen et al., 2002), and the other is NDVI-based linear mixture approaches (Gutman & Ignatov, 1998; Gallo et al., 2001, 2005; Jiang et al., 2010).

Multispectral mixture approaches use reflectance of fully vegetated land and bare soil in multiple spectral bands to derive FVC or GVF (DeFries et al., 1999; Hansen et al., 2002). These approaches need endmember libraries to distinguish soil/vegetation and their subclasses. Their disadvantages include: (a) spectral signature of endmembers are hard to define or identify (may vary from pixel to pixel), (b) extensive training data are needed for each endmember, and (c) many such approaches need a surface reflectance model, which in turn, needs atmosphere corrected surface reflectance. Both are very complicated and computationally expensive, and thus may introduce the chance of errors.

NDVI-based linear mixture approaches involve the use of the measured NDVI values and a linear mixture model with two endmembers representing fully vegetated land surface and bare ground respectively (Gutman and Ignatov, 1998, Gallo, 2001, Jiang et al, 2010), to calculate GVF as formulated in Equation (3.1),. These approaches directly link the real-time observed NDVI to GVF via a simple formulation that helps reduce the distortion to the real-time signal in NDVI and requires significantly fewer parameters than the multispectral mixture approaches (Jiang et al., 2010). The disadvantages of such approaches include: (a) NDVI angular anisotropy has to be accounted for, and (b) NDVI should be brought to the same geometry of observations.

Both the MODIS vegetation fraction (continues field) product (DeFries et al., 1999; Hansen et al., 2002) and the EUMETSAT land GVF product derived from SEVIRI ((SAF/LAN/UV/PUM_VEGA/2.1) utilized the multispectral mixture approaches. Two sets of NOAA NESDIS AVHRR-based GVF products utilized the NDVI-based linear mixture approach. The GVF dataset that is currently used in NCEP forecast model is a monthly climatology data derived by Gutman and Ignatov (1998) using 5 years NDVI data at 0.144º resolution from the NOAA AVHRR. NESDIS has recently generated a AVHHR-based, near real-time weekly dataset of GVF from 1982 through present with global coverage (Jiang et al. 2010). The new global GVF data sets include the multiyear GVF weekly climatology and the real-time weekly GVF. This dataset has the same spatial resolution as the old monthly GVF, however, provide an overall higher vegetation value, real-time surface vegetation information, and numerous other improvements (Jiang et al., 2010)

In this study, we follow the general approach by Gutman and Ignatov (1998) and Jiang et al (2010), as described in Equation (3.1). In addition to the above mentioned advantages, this approach is to follow the heritage of NOAA method, and thus it will have a long history of similar data from previous and existing polar-orbiting satellites, and also be easy to create merged products from ABI and polar-orbiting satellites in the future.

In the formula (3.1) *NDVI* is the observed NDVI, $NDVI_{max}$ is the maximum NDVI corresponding to 100% vegetation cover, and $NDVI_{min}$ is the minimum NDVI corresponding to 0% vegetation cover or bare soil. $NDVI_{max}$ and $NDVI_{min}$ are global parameters independent of location or land cover type. All three terms *NDVI*, $NDVI_{max}$ and $NDVI_{min}$ are top of the atmosphere values. This approach to estimate the green vegetation fraction was adopted for generation of the GVF product from GOES-R ABI.

Estimating GVF faces two principal challenges. First, it has to be considered that NDVI depends on the observation geometry. This occurs due to different angular anisotropy of reflectance in the visible and near-IR spectral bands contributing to NDVI. Many applications implicitly assume that angular effects on NDVI are negligible (Zhou et al., 2001; Schwartz et al., 2002). However, it has been demonstrated that TOA NDVI depends on atmospheric path scattering and land surface bidirectional reflective properties. (Gao et al., 2002). To achieve consistent retrievals of GVF both in space and time a proper mechanism to correct NDVI for angular effects prior to using it in formula (3.1.) had to be developed. The second challenge consists in accurate determination of the values of $NDVI_{max}$ and $NDVI_{min}$ which are the major parameters controlling the algorithm.

In the development of the GVF algorithm for GOES-R ABI we heavily relied on the data from MSG SEVIRI as a proxy to ABI data. Similar to ABI SEVIRI is a geostationary satellite instrument which provides observations in the visible and near-infrared spectral range and thus can be used to derive NDVI and GVF. A detailed description of the GVF algorithm development activities is given in the following section. This includes the work on the development of the NDVI bidirectional correction algorithm and the approach to estimate global minimum and maximum NDVI values.

## 3.4.2 Mathematical Description of the GVF Algorithm

### 3.4.2.1 Observed NDVI Angular Anisotropy

Proper correction of NDVI for angular anisotropy is a critical step towards generating consistent in space in time estimates of GVF. In the analysis of NDVI angular anisotropy as well as in the development of an algorithm to correct for NDVI angular anisotropy and to derive GVF we have used observations from the Spinning Enhanced Visible and Infrared Imager (SEVIRI) sensor onboard the European Meteosat Second Generation (MSG) satellite as the GOES-R ABI prototype. MSG is a geostationary satellite operated by EUMETSAT and positioned over equator at $0^o$ longitude. The SEVIRI instrument provides observations in 12 spectral bands including observations in the visible red and in near infrared spectral range. The latter feature

allows for using MSG SEVIRI data to estimate NDVI and, hence GVF. Detail information on SEVIRI data is provided in section 4.1

To study the angular anisotropy of the TOA NDVI we have developed a special system to visualize diurnal time series of SEVIRI-observed reflectances, brightness temperatures and NDVI and to select time series that were not affected by clouds. The system plots time series of half-hourly SEVIRI observations for a specified location and date. Discrimination between cloud-clear and cloud-contaminated time series is performed interactively by qualitative evaluation of the smoothness of time series of the observed reflectance, infrared brightness temperature and NDVI.

The visualization system was used to examine MSG SEVIRI half-hourly images obtained during one year time period, from Feb 2007 to Feb 2008. Data for two days of every month have been examined to identify cloud-clear time series. Overall about 880 daily time series of reflectance and NDVI were identified and saved. When generating this dataset we have try to cover as evenly as possible the whole domain of SEVIRI and incorporate observations characterizing all land major land surface cover types. Locations of selected and saved cloud clear diurnal time series are shown in the map in Figure 3.2

Figure 3.2. Locations where clear NDVI daily records were acquired from the SEVIRI dataset.

Examination of diurnal time series of clear sky NDVI has revealed a strong angular anisotropy inherent to NDVI values (Figure 3.3 and 3.4). It was found that in some cases changing solar zenith angle during the day causes up to 0.4 change in the observed TOA NDVI. The effect of the solar-satellite relative azimuth on NDVI was smaller, but may still cause a change of about 0.1. The NDVI dependence on relative azimuth may result in an asymmetry in the NDVI daily change. Overall angular anisotropy in NDVI increased with increasing NDVI values.

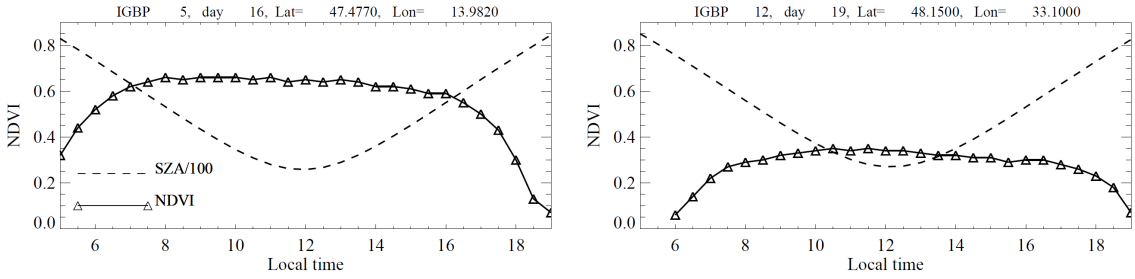


Figure 3.3. Examples of NDVI daily change (as function of solar zenith angle/local time) from July 2007 MSG-SEVIRI cloud-clear data. The vegetation types are mixed forest (left panel) and cropland (right panel).

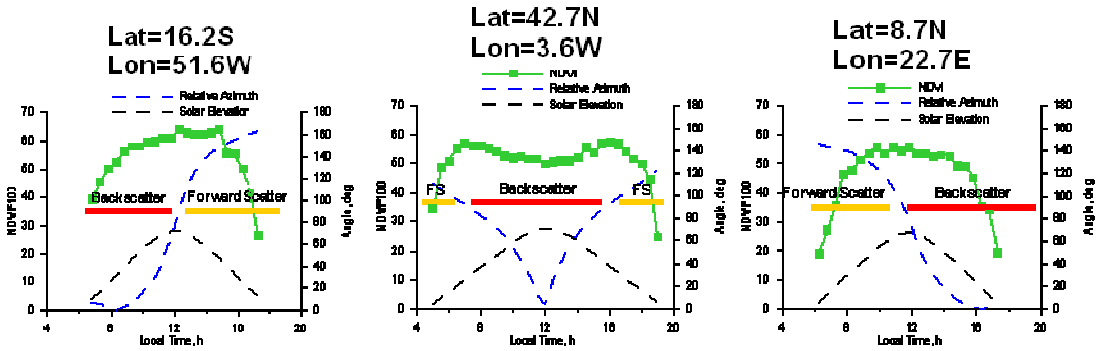


Figure 3.4. Effect of solar-satellite relative azimuth angle on NDVI daily change (as local time) from MSG-SEVIRI cloud-clear data.

In order to understand how atmospheric effects influence the NDVI anisotropy seen by satellites, the “second simulation of a satellite signal in the solar spectrum” (6S) code(reference for 6S model needed) and Boston University’s BRDF model were used to simulate the top of canopy (TOC) and TOA reflectance and NDVI with aerosol optical depth (AOD) of 0.05, 0.15, 0.25 and 0.45, respectively. Three different vegetation types (dense broadleaf tree-shrubs, dense needle leaf trees-shrubs, and dense grass like vegetation - crops) and three different soil types (smooth dark soil, smooth bright soil, rough bright) were used in this work.

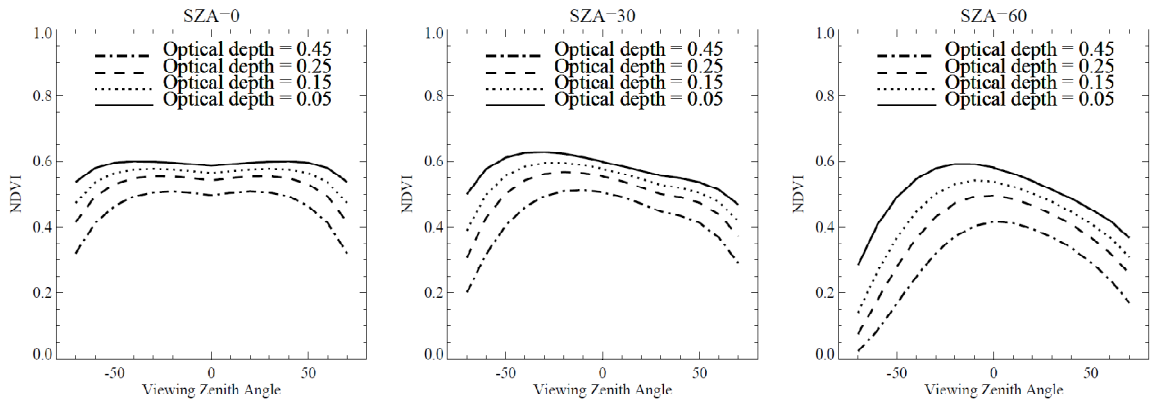


Figure 3.5. Simulated TOA NDVI as function of view zenith angle, with the aerosol optical depth of 0.05, 0.15, 0.25, and 0.45. The vegetation type used in this simulation is dense needleleaf trees-shrubs.

Figure 3.5 shows that the magnitude of NDVIs generally decreases with the increase of AOD. With the same amount of AOD, bidirectional NDVI at TOA has a dome shape when canopy was measured from the near-nadir view to larger view angles. This means that as the viewing or solar zenith angle increases, the atmospheric contribution to TOA reflectance increases and thus causes a TOA bidirectional NDVI decrease.

These results indicate that although geostationary satellites making repeat observation over a given region can provide high temporal resolution data, the different satellite viewing zenith angles for different locations on Earth may bring large uncertainties to GVF, e.g., the NDVI measured from larger viewing zenith angles will be underestimated even at the overhead sun condition. In addition, if original NDVI values are used in calculating GVF, GVF will also change with observation geometry and thus cause substantial spurious diurnal variations in the derived GVF. GVF is supposed to characterize vegetation cover properties and should not depend on the observation geometry. Therefore, to provide consistent estimates of GVF all TOA NDVI measurements should be brought to a reference geometry before using them in formula (3.1) to estimate GVF.

### 3.4.2.2 NDVI Angular Anisotropy Model

Kernel-driven models are widely used to reproduce bidirectional reflective properties of the land surface reflectance and to calculate the surface albedo (Roujean et al., 1992; Wanner et al., 1995; Lucht et al., 2000). Some of the developed BRDF models are quite simple and are based on purely empirical considerations (e.g. Walthall et al., 1985; Nilson and Kuusk,1989) . Other models are more complicated and have some physical background. The most widely used semiempirical BRDF models are those of Roujean et al. (1992), Wanner et al. (1995) and Lucht

et al. (2000). The kernel functions in these models are based on simplified physical parameterizations of the light scattering and reflection processes over vegetated terrain.

The kernels of semiempirical BRDF models represent basic scatter types: isotropic scattering, radiative transfer-type volumetric scattering as from horizontally homogeneous leaf canopies, and geometric-optical surface scattering as from scenes containing 3-D objects that cast shadows and are mutually obscured from view at off-nadir angles (Lucht et al., 2000).

A linear kernel-driven BRDF model developed by Roujean et al. (1992) incorporates two kernel functions and three coefficients (or kernel weights) and has the following form:

$$BRDF(\theta_S, \theta_V, \varphi) = k_0 + k_1 * f_1(\theta_S, \theta_V, \varphi) + k_2 * f_2(\theta_S, \theta_V, \varphi) \quad (3.2)$$

In equation (3.2) the two functions $f_1$ and $f_2$ were derived separately from elementary photometric models, representing volume-scattering and geometric scattering effects, respectively. They are functions of zenith angles $\theta_S$ for the Sun and $\theta_V$ for the sensor, and the relative azimuth $\varphi$ between the Sun and the view directions. The retrieved coefficients $k_i$ ($i$= 0, 1, 2), weights for the kernels and obtained from model inversion against satellite measurements, represent intrinsic surface properties. Coefficient $k_0$ is a nadir-zenith reflectance (a constant corresponding to isotropic reflectance), whereas $k_1$ and $k_2$ quantify the volume scattering and the geometric-optical surface scattering of the surface, respectively.

Since these BRDF models are linear models, they can be inverted analytically. Both the MODIS BRDF/Albedo (Schaaf et al., 2002) and the ADEOS-POLDER BRDF products (Leroy et al., 1997; Hautecoeur and Leroy, 1998) utilized kernel-driven BRDF models. In the MODIS BRDF/Albedo algorithm, the reciprocal RossThick-LiSparse model was used (Lucht et al. 2000). In the ADEOS-POLDER BRDF product, the Roujean BRDF model (Roujean et al., 1992) was used.

In this study we have used a similar kernel-based approach to parameterize NDVI angular anisotropy and have proposed a simple analytical model relating NDVI to the observation geometry.

From the physical point of view, the approach involving atmospherically corrected and BRDF-adjusted reflectances to calculate TOC NDVI and, further on, GVF appears more justified. This technique is extensively used for generating vegetation-related parameters from MODIS data. The reasons we chose to follow an empirical approach to NDVI anisotropical correction are as follows.

First, atmospheric correction needs aerosol parameters to be accurately defined and the latter are often poorly known. There is no specified atmospheric correction team as MODIS land team to convert TOA reflectance to TOC reflectance in current GOES-R land team.

Second, BRDF correction is performed with a semi-empirical kernel-driven model similar to the one used in our algorithm to correct NDVI. The required accuracy of GVF estimates ranges from

10% to 20% depending on the satellite view angle. To achieve this accuracy the normalized reflectance should be defined with an error of less than 2%. It hardly reasonable to expect that a simple BRDF model can reproduce reflectance so accurate in both spectral bands for the whole variety of different land surface cover types within the full range of viewing and illumination geometries inherent to observations from geostationary satellites.

Third, if the specified precision for the surface reflectance is 0.08 as mentioned in GOES-R ABI land surface albedo ATBD, uncertainties in NDVI range within 0.15 to 0.4 for most scenarios and corresponding uncertainties in GVF range within 20% to 60% (instead of 10%-20% as required by F&PS document). In the latter estimates NDVI and GVF uncertainties were calculated from the surface uncertainty using a simple error propagation formula. It was assumed that NDVI min and max values were equal to 0.0 and 0.7 respectively and were defined with the accuracy of 0.05. The surface reflectance uncertainty was taken equal to 0.08.

Considering all issues mentioned above we believe that at this time the proposed empirical approach to NDVI anisotropical correction is the optimal choice.

To correct NDVI for the angular anisotropy, a simple kernel-driven model has been proposed:

$$NDVI(\theta_S, \theta_V, \varphi) = NDVI(0,0,0)\,[1 + C_1 f_1 + C_2 f_2] \tag{3.3}$$

Where $f_1$ and $f_2$ are kernel functions, $C_1$ and $C_2$ are kernel weights, $\varphi$ is relative azimuth, $\theta_S$ is solar zenith angle and $\theta_V$ is satellite zenith angle.

In this equation, the first kernel function is meant to characterize NDVI change with solar and satellite zenith angle:

$$f_1 = (\tan\theta_S + \tan\theta_V), \tag{3.4}$$

whereas the second kernel function reproduces NDVI change with the relative solar-satellite azimuth angle:

$$f_2 = (\cos\varphi + 1)^2 (\tan\theta_S \tan\theta_V)^{1/2}. \tag{3.5}$$

The NDVI anisotropy model assumes reciprocity of viewing and illumination angles. Both kernel functions turn into zero for the overhead sun and nadir observations conditions.

Two kernel weights $C_1$ and $C_2$ were determined from SEVIRI clear sky observations using the following empirical approach. For two observations taken over the same scene during one day at different illumination conditions NDVI (0,0,0) should be the same, hence we have

$$NDVI(\theta_{S1}, \theta_{V1}, \varphi_1) /[1 + C_1 f_{11} + C_2 f_{21}] = NDVI(\theta_{S2}, \theta_{V2}, \varphi_2) /[1 + C_1 f_{12} + C_2 f_{22}] \quad (3.6)$$

Where $f_{11} = (\tan\theta_{S1} + \tan\theta_{V1})$, $f_{12} = (\tan\theta_{S2} + \tan\theta_{V2})$, $f_{21} = (\cos\varphi_1 + 1)^2 (\tan\theta_{S1} \tan\theta_{V1})^{1/2}$, and $f_{22} = (\cos\varphi_2 + 1)^2 (\tan\theta_{S2} \tan\theta_{V2})^{1/2}$. The observation geometries are $\theta_{S1}, \theta_{V1}, \varphi_1$ for the first measurement, and $\theta_{S2}, \theta_{V2}, \varphi_2$ for the second measurement. Since the target is the same, the satellite zenith angle does not change: $\theta_{V1} = \theta_{V2}$.

Reformulate (3.6) we have:

$$NDVI(\theta_{S1}, \theta_{V1}, \varphi_1) - NDVI(\theta_{S2}, \theta_{V2}, \varphi_2) = \quad (3.7)$$

$$C_1 [ NDVI(\theta_{S2}, \theta_{V2}, \varphi_2) f_{11} - NDVI(\theta_{S1}, \theta_{V1}, \varphi_1) f_{12}] +$$

$$C_2 [ NDVI(\theta_{S2}, \theta_{V2}, \varphi_2) f_{21} - NDVI(\theta_{S1}, \theta_{V1}, \varphi_1) f_{22}]$$

Hence we obtain a system of linear equations to determine coefficients $C_1$ and $C_2$ based on a set of pairs of observations taken over the same scene but under different illumination conditions. In this reformulated equation, all are known except $C_1$ and $C_2$. By using multiple linear regression, we can derive $C_1$ and $C_2$ based on a set of pairs of observations taken over the same scene but under different illumination conditions.

To derive C1 and C2 we have used cloud-clear time series of NDVI observations with SEVIRI from the dataset presented above. . About 5% of all 800+ accumulated clear sky NDVI daily time series were used to determine coefficients $C_1$ and $C_2$ whereas the rest of the data have been used to assess the accuracy of the developed algorithm. The best fit to the observed NDVI has been obtained with the following values of the two coefficients:

C1 = -0.0723
C2 = -0.0101

Note that $C_1$ and $C_2$ are global values for every pixel.

### 3.4.2.3 NDVI Angular Anisotropy Model Testing

Assessment of the performance of the NDVI angular model is presented in this section. Criteria characterizing the validity of the NDVI anisotropy model include (1) Ability of the model to accurately reproduce the observed NDVI diurnal change; and (2) Decrease of scatter in diurnal time series of corrected NDVI (or NDVI brought to a common sun-satellite geometry) as compared to the original observed NDVI. The evaluation of the NDVI angular anisotropy model is based on these two criteria.

### 3.4.2.3.1 NDVI observed versus NDVI predicted

Once the NDVI angular anisotropy model is defined, one observation of NDVI during the day can be used to predict NDVI that will be observed at any other time of the day. The following experiments have utilized cloud-clear NDVI diurnal time series. We have used one NDVI observation close to noon and simulated SEVIRI-observed NDVI during the rest of the day:

$$NDVI(\Theta_{S2}, \Theta_{V2}, \varphi_2) = \quad (3.8)$$
$$NDVI(\Theta_{S1}, \Theta_{V1}, \varphi_1) / [1 + C_1 f_{11} + C_2 f_{21}] * [1 + C_1 f_{12} + C_2 f_{22}],$$

where $NDVI(\Theta_{S1}, \Theta_{V1}, \varphi_1)$ is NDVI observed at the local noon, and $NDVI(\Theta_{S2}, \Theta_{V2}, \varphi_2)$ is predicted NDVI at any other time with cloudy clear condition within the same day. Since the target is the same, $\Theta_{V1} = \Theta_{V2}$.

Figure 3.6 presents two examples of the observed and simulated NDVI. In both cases the model reproduces the diurnal change of NDVI quite well. In both examples the model has been applied for observations with solar elevation above $30^0$. The model performance was found to degrade substantially at lower solar elevation angles. This, however is does not present a critical issue since quantitative accuracy and precision criteria for GVF are specified only for the solar zenith angle below $67^0$ and for satellite zenith angle below $70^0$.

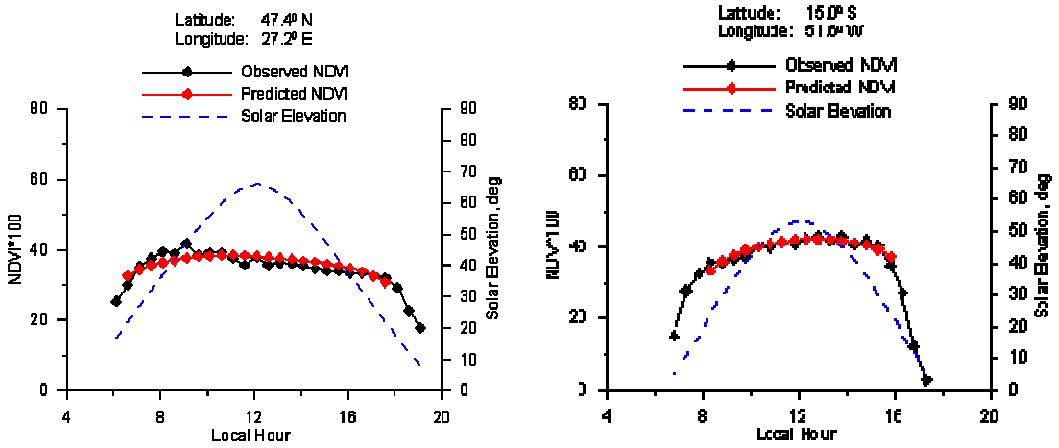


Figure 3.6. Comparison of NDVI daily change between original observed SEVIRI NDVI and predicted NDVI using the angular anisotropy model.

Diurnal time series NDVI that were collected for about 880 locations in Europe, Asia and Africa within the SEVIRI domain (mentioned in section 3.4.2.1, figure 3.2) have been used to test the accuracy of the model. For each NDVI diurnal time series, we have calculated the value of the root mean square error (RMSE). The mean RMSE over all 880 cases in the dataset was equal to 0.032.

### 3.4.2.3.2 NDVI observed versus NDVI corrected to a reference geometry

Figure 3.7 illustrates the results of NDVI angle correction. Given every individual $NDVI(\Theta_{S1}, \Theta_{V1}, \varphi_1)$ observation within a day, corresponding NDVI that is brought (corrected) to the reference sun-satellite geometry, $NDVI(\Theta_{S2}=45°, \Theta_{V2}=45°, \varphi_2=90°)$, can be calculated using formula (3.8). Figure 3.7 shows some individual comparison.

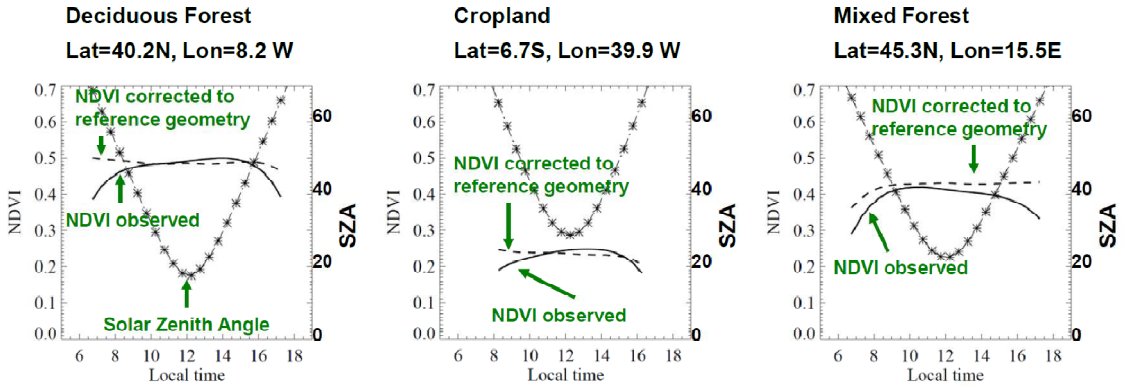


Figure 3.7. NDVI observed versus NDVI corrected to a reference sun-satellite (or viewing-illumination) geometry.

The effect of NDVI angular correction is evaluated by comparing the root mean square difference (RMSD) of NDVI in the diurnal time scale. The RMSD is calculated as,

$$RMSD = \sqrt[2]{\frac{\sum_{i=1}^{n}(NDVI_i - \overline{NDVI})^2}{n}} \tag{3.9}$$

Where $NDVI_i$ is either the NDVI corrected to the reference geometry or the original measured one in a diurnal time scale for one pixel, n is the total number of clear sky measurements in a whole day for that pixel, and $\overline{NDVI}$ is the corresponding mean NDVI (calculated from angular corrected NDVI or original measured NDVI) in that day. The detail procedure is as follows. First, hourly clear-sky NDVI (angular corrected and original) for every location are collected. Second the diurnal NDVIs RMSD is calculated. Last, the frequency distribution of RMSD for all pixels is showed in Figure 3.8.

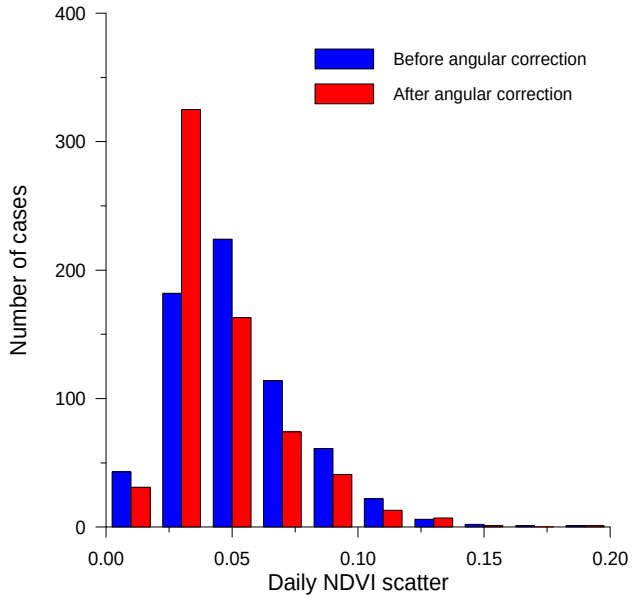


Figure 3.8. The Statistics of RMSD in daily NDVI records before and after angular correction (cloud clear daily NDVI time series used). The 880 daily time series of SEVIRI NDVI are used (mentioned in section 3.4.2). The x axis is NDVI RMSD value.

The values in blue in Figure 3.8 are the results from original observed NDVI daily record. The values in red are the results from corrected NDVI. Low RMSD values means less diurnal changes. After the angular correct, there are significant more cases of small RMSD, which means that NDVI brought to the reference sun-viewing geometry shows less scatter at daily time scale as compared to the original NDVI. However, anisotropical correction reduces the scatter in NDVI daily time series but does not eliminate the diurnal change completely**.**

### 3.4.2.4 Approach to determine $NDVI_{max}$ and $NDVI_{min}$

To calculate GVF with a linear mixture approach based on NDVI, the values of endmemebrs representing fully vegetated land surface ($NDVI_{max}$) and completely non-vegetated land surface ($NDVI_{min}$) should be determined. We have used an empirical approach to determine the values of both $NDVI_{min}$ and $NDVI_{max}$.

To estimate the NDVI value corresponding to completely vegetated land surface we have processed MSG SEVIRI half-hourly full disk images collected during the years of 2007 and 2008 and generated weekly maximum NDVI composited images. Weekly maximum NDVI values were corrected for the angular anisotropy with the model presented above and were brought to a reference geometry of observation ($\theta s$ = 45°, $\theta v$ = 45°, $\varphi$ = 90°). Corrected NDVI values were then used to generate the frequency distribution of NDVI. The value of $NDVI_{max}$ was assumed equal to the value of 95th percentile of NDVI frequency distribution. The 95th percentile corresponds to NDVI value of 0.59 (Figure 3.9).

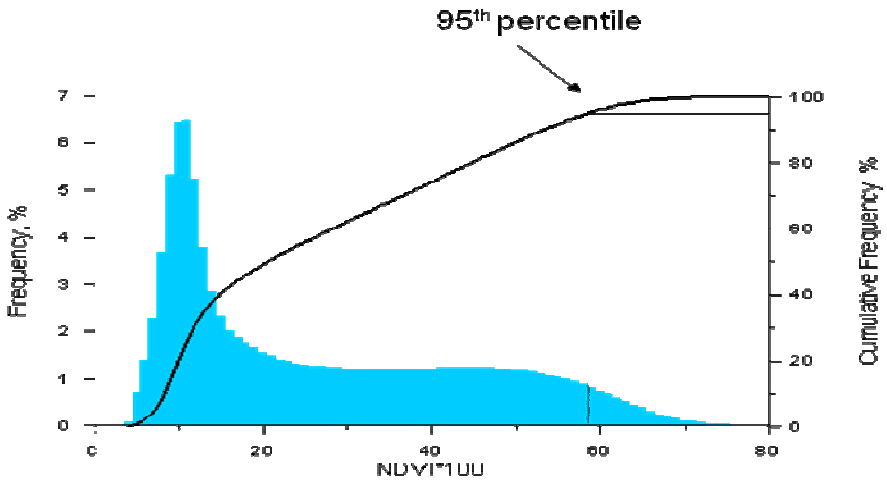


Figure 3.9. NDVI frequency distribution for the full disk data.

The $NDVI_{min}$ value was determined through the following procedure. A test site in Sahara desert (Figure 3.10) was selected to represent a completely non-vegetated land-surface. NDVI frequency distribution over this area was derived from NDVI weekly maximum composited maps. The value of NDVI for non-vegetated land surface was taken equal to 95th percentile of NDVI frequency distribution in Sahara desert ($NDVI_{min}$=0.13).

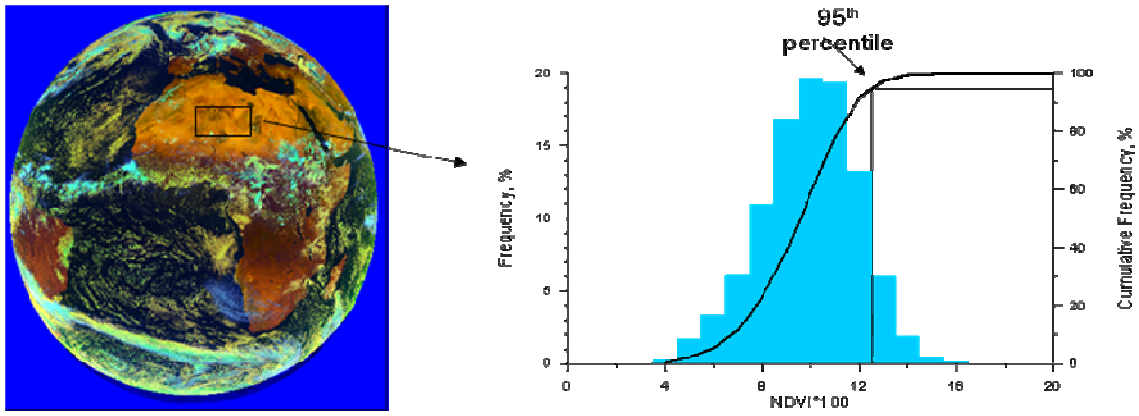


Figure 3.10. NDVI frequency distribution for a test site in Sahara desert (barren soil). NDVI is corrected for anisotropy and brought to the reference geometry ($\Theta s = 45°$, $\Theta v = 45°$, $\varphi = 90°$)

Setting $NDVI_{max}$ and $NDVI_{min}$ equal to correspondingly 95 percentile of the global NDVI statistics and 95% of NDVI statistics over desert areas means that observed values of NDVI may both exceed $NDVI_{max}$ or turn less than $NDVI_{min}$. To avoid reporting unrealistic values in the product GVF, the derived values of GVF are constrained to the [0;1] range.

### 3.4.3 Summary of the Algorithm

The GOES-R ABI GVF product is derived from GOES-R ABI NDVI product. Only cloud/snow clear cases are considered in GVF retrievals. Linear mixture model is used to estimate GVF from NDVI. NDVI is corrected for angular anisotropy using a kernel-driven model. NDVI anisotropy model kernel weights as well as endmember values for the GVF model ($NDVI_{max}$ and $NDVI_{min}$) were determined empirically from SEVIRI clear sky data.

We emphasize that all the results discussed to this point assume perfect cloud and snow detection. That is, all these results are for truly cloud and snow clear pixels. Pixels that are affected by clouds/snow or that cannot be used to estimate GVF for any other reason will be flagged and filled with gaps. Correspondingly no GVF value will be derived and/or assigned to these pixels. At current stage of our algorithm development, there is no plan to make hourly GVF maps a spatially-continuous product.

## 3.5 Algorithm Output

Output of the GVF algorithm consists of the dataset of scaled GVF values and the other dataset of corresponding Quality Control flags for each pixel (see Table 3.4). Scaled GVF values will be provided as 2-byte integer for every pixel where GVF retrieval was performed. All other pixels where GVF retrieval was not attempted (e.g., pixels covered with cloud, snow, having insufficient daylight or lacking valid NDVI retrievals) will be assigned a fill in value of 255. The QC flag is meant to explain the reason the GVF value for the pixel is not available.

*Table 3.4. Algorithm output data*.

| Name | Type | Description | Dimension |
|---|---|---|---|
| GVF values | output | Scaled GVF values:<br>(GVF+1)*100=100*GVF+100 | grid (xsize, ysize) |
| QC flags | output | Quality control flags for each pixel of the scanning mode:<br>Land, cloudiness, sensor data quality, day/night, large view zenith, snow covered surface, etc. | grid (xsize, ysize) |

The QC flag is a 2-byte integer value provided for every pixel. The structure of the QC flag for the GVF product is defined in Table 3.5. The first bit of the first byte of the QC provides general information on the availability and quality of the derived GVF value (0(good quality)/1(bad quality)). If GVF defined as bad quality, the user is suggested to examine the second byte, which specifies the reason for GVF data unavailability or bad quality.

The bits in the second byte of the QC give each specified standards we used to define whether this pixel pass our specification. The quality flag is initialized to invalid (1) for all pixels. If the pixel is determined to be a space pixel (satellite zenith angle is greater than 70 degree), the quality flag remains “invalid due to space pixel” (bit 0 of byte 2 is 1). If the pixel is an ocean/water pixel, the quality flag is set to “Invalid pixel due to being outside of land” (bit 1 of

byte 2 is 1). If the pixel is a land pixel with a solar zenith angle greater than 67 degrees, the quality flag is set to “Invalid pixel due to being outside of sensor zenith range/night” (bit 2 of byte 2 is 1). If the pixel is a land pixel at day time with cloudy, the quality flag is set to “Invalid pixel due to cloud” (bit 3 of byte 2 is 1). If the pixel is a land pixel at day time without cloudy but has snow, the quality flag is set to “Invalid pixel due to snow” (bit 4 of byte 2 is 1). If the pixel is a land pixel at day time without cloudy and now, but has an invalid NDVI value, the quality flag is set to “Invalid pixel due to invalid input data” (bit 5 of byte 2 is 1).

After all of above mentioned tests have been completed, two further tests on the quality of the GVF algorithm retrieval are performed. The first is to check if the retrieved pixel has solar zenith angle greater than 55 degrees. If the retrieved pixel has solar zenith angle greater than 55 degrees, then the quality flag is set to “Reduced quality” (bit 6 of byte 2 is 1). The second test is to check if the retrieved pixel has satellite zenith angle greater than 55 degrees. If the retrieved pixel has satellite zenith angle greater than 55 degrees, then the quality flag is set to “Reduced quality” (bit 7 of byte 2 is 1).

If neither of these criteria listed in byte 2 are met, then the quality flag for the pixel is set to “Good quality” (bit 0 of byte 1 is 0).

*Table 3.5. GVF algorithm defined quality control flags* (*subject to change)*

| Byte | Bit | Description |
|---|---|---|
| *Ancillary Data Flags* | | |
| 1 | 0 | [1]Good quality (0) / Bad quality (1) |
| 1 | 1 | |
| 1 | 2 | |
| 1 | 3 | |
| 1 | 4 | |
| 1 | 5 | |
| 1 | 6 | |
| 1 | 7 | |
| 2 | 0 | [2]Global pixel(0) / Corner pixel(1) |
| 2 | 1 | Land (0) / Ocean (1) |
| 2 | 2 | Day (0) / Night (1) |
| 2 | 3 | Clear (0) / Cloudy (1) |
| 2 | 4 | No snow (0) / Snow (1) |
| 2 | 5 | Valid NDVI (0) / Invalid NDVI(1) |
| 2 | 6 | Solar zenith angle smaller than 55° (0) / between 55° ~ 67° (1) |
| 2 | 7 | Satellite zenith angle smaller than 55° (0) / between 55° ~ 70° (1) |

[1]Good quality data means GVF derived from valid NDVI with solar and satellite zenith angle smaller than 55°. Bad quality data means GVF derived from valid NDVI with solar zenith angle between 55° ~ 67° and satellite zenith angle between 55° ~ 70°.

[2]Global pixel is for pixel with satellite zenith angle <=90.

In addition to the pixel level GVF values and quality control flags, metadata will be provided for the GVF product describing the common and GVF specific information about the product. The

GOES-R AWG and the Land Team recommends the following metadata (Table 3.6) to be provided for the ABI GVF products.

*Table 3.6. Metadata defined for the GVF product file*

| Metadata | type | Definition |
|---|---|---|
| Date | common | Beginning and end dates of the product |
| Time | common | Beginning and end times of the product |
| Bounding Box 1 | common | Resolution, number of rows, number of columns |
| Bounding Box 2 | common | Byte per pixel, data type, byte order information, location of box relative to nadir |
| Product Name | common | The ABI GVF product name |
| Ancillary Data Used | common | Ancillary data name, version |
| Satellite | common | GOES-R satellite name |
| Instrument | common | ABI |
| Altitude | common | Altitude of the satellite |
| Position | common | Latitude and longitude of the satellite position |
| Version | common | Product version number |
| Compression | common | Data compression type (method) used |
| Location | common | Location where the product is produced |
| Contact | common | Contact information of the producer/scientific supporter |
| document | common | Citations to documents (i.e., ATBD) |
| | | |
| Product Unit | GVF | Unitless |
| Statistics | GVF | Mean and standard deviation of all the available GVFs |
| Good pixels | GVF | Number of pixels the retrieved GVFs are with the LZA smaller than 55 degree (cloudless land surface pixels) |
| Total Pixels | GVF | Total pixels GVFs are retrieved (cloudless land surface pixels) |

# 4 TEST DATASETS AND OUTPUTS

## 4.1 Simulated/Proxy Input Datasets

Observations from the Spinning Enhanced Visible and Infra-red Imager (SEVIRI), onboard the European Meteosat Second Generation (MSG) satellite, are used as proxy for GOES-R ABI in the GVF algorithm verification/validation. Both MSG and GOES-R are geostationary satellites. SEVIRI spectral channels in the visible and near infrared spectrum are close to ABI channels This section describes the proxy and validation datasets used in assessing the performance of the GVF.

Table 4.1 provides a channel comparison of the visible and near infrared channels on those two instruments.

*Table 4.1. Channel comparison of ABI and SEVIRI as proxy*

| Sensor | Channel No. | Wavelength Center (μm) | Band width (μm) | Sensor Noise (SNR) | Spatial Resolution |
|---|---|---|---|---|---|
| **ABI** | 2 | 0.64 | 0.59 – 0.69 | 300:1@100% albedo | 0.5 km |
| | 3 | 0.865 | 0.846 – 0.885 | 300:1@100% albedo | 1 km |
| **SEVIRI** | 1 | 0.635 | 0.56 – 0.71 | 10.1 @ 1% albedo | 3 km |
| | 2 | 0.81 | 0.74 – 0.88 | 7.28 @ 1% albedo | 3 km |

### 4.1.1 SEVIRI Data

MSG SEVIRI has 11 spectral bands centered in the visible and in the infrared portion of the spectrum. The spatial resolution of MSG SEVIRI observations is 3 km; observations are made at 15 minutes interval. Close similarity of SEVIRI and ABI makes it reasonable to use SEVIRI observations in the development and testing of the GVF algorithm.

Since the year 2007 full disk SEVIRI observations are routinely acquired and archived at NESDIS through the Man-computer Interactive Data Access System (McIDAS) system. A complete archive of MSG SEVIRI data since the end of 2004 is available at the University of Wisconsin Space Science and Engineering Center (SSEC). Figure 4.1 presents an example of a full-disk SEVIRI image.

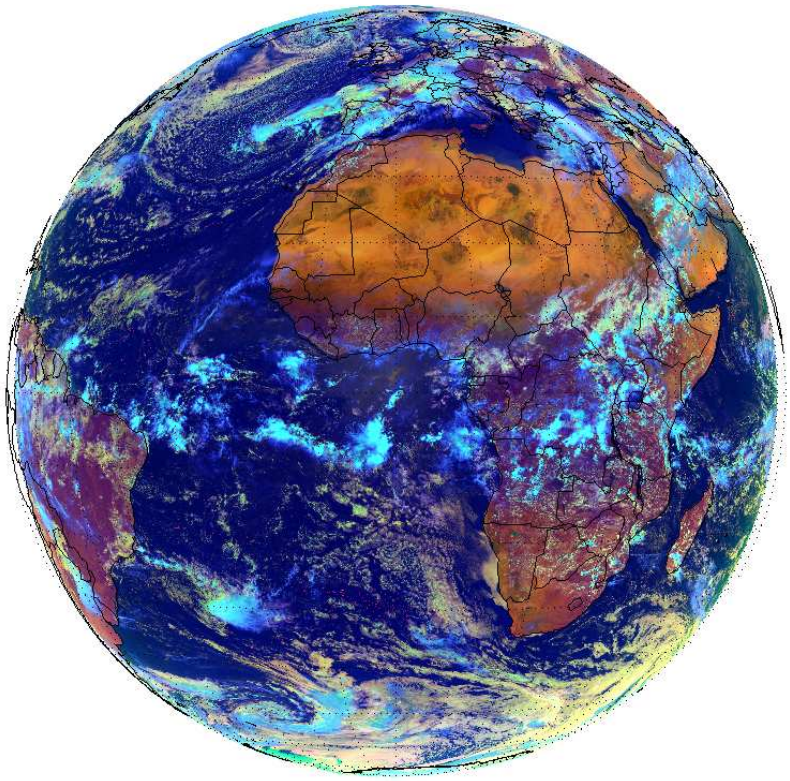

Figure 4.1. Full disk false color image from SEVIRI for 12:15 UTC on April 9, 2008. The image is composed of channel 3 reflectance at 1.6 µm (in red), channel 1 reflectance at 0.6 µm (in green) and inverted channel 9 brightness temperature (in blue).

## 4.2 Output from Simulation/Proxy Datasets

### 4.2.1 Output Results

The developed algorithm has been applied MSG SEVII data to generate GVF full disk image products since March 2007. To date, SEVIRI NDVI and GVF results are available every 30 minutes for day 1 – day 63 and day 183 – day 245, 2008 and 2009. The mainframe output products include cloud mask, angular corrected NDVI, GVF and other QC information in binary format. Figure 4.2 shows an example of the GVF instantaneous product over cloud free land areas. This image is for the day 141 in 2007.

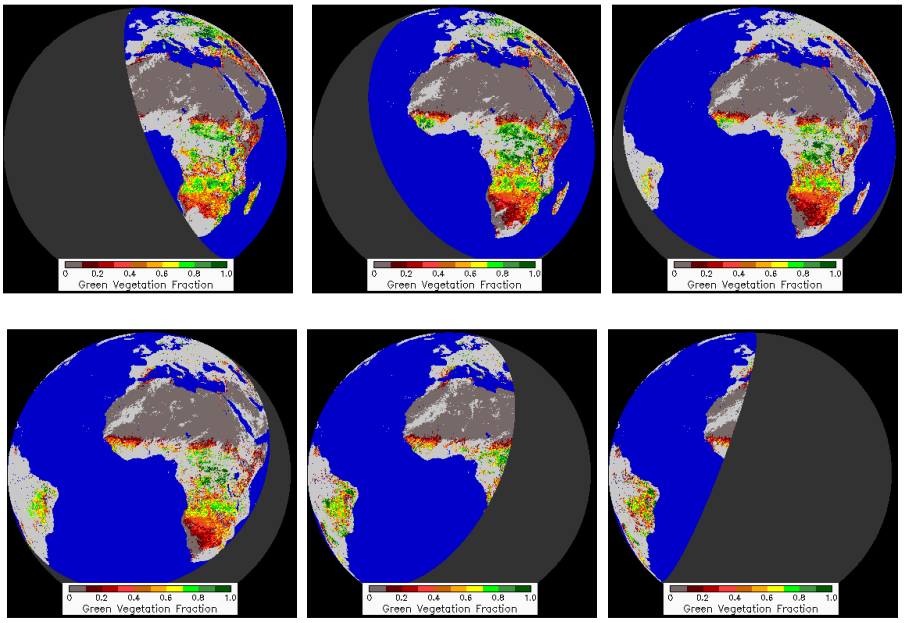


Figure 4.2. Example GVF calculated from angular corrected NDVI, date: 2007141. Light gray: clouds, dark gray: solar zenith angle above 70 degree.

### 4.2.2 Precisions and Accuracy Estimates

Potential for quantitative validation of the GVF product is limited due to the fact that no *in situ* observations of GVF are available. As a result the validity of the product can only be assessed indirectly through the analysis of GVF spatial distribution and temporal change. Particular criteria which are indicative of the validity of GVF retrievals are as follows. The GVF product should demonstrate 1) adequate reproduction of GVF seasonal change; 2) adequate reproduction of GVF geographical distribution; 3) small spurious diurnal change of derived GVF, which means that diurnal change should be consistent with precision specification; and 4) small day-to-day change of the derived GVF (should be within precision specification for GVF). The first two criteria can be used to only qualitatively characterize the performance of the algorithm. The latter two criteria can be used to estimate the precision of GVF retrievals.

It is identified that major risks in the GVF product quality may be associated with the following aspects:

- Inaccurate cloud identification (missed clouds)
- Inaccurate snow identification
- Cloud shadows
- Limited accuracy of NDVI angular anisotropy model
- Variation in $NDVI_{min}$
- Sensor calibration, image navigation, and channel co-registration.

### 4.2.3 Error Budget

As stated in the previous section, requirements for both GVF accuracy and precision are set at 0.10 GVF unit for observations at satellite zenith angles below 55 degrees and at 0.20 GVF for satellite zenith angles ranging from 55 to 70 degrees.

### 4.2.4 Validation Result from the SEVIRI Test Data

#### 4.2.4.1 Software Verification

To test the software readiness, the output of the GVF algorithm on the AWG developer's Linux machine was compared to the output of the algorithm implemented on a Linux machine in the collaborative environment within the AIT's Framework. SEVIRI data for 12:15 and 12:45 UTC on July 1, 2008 along with cloud cover mask for these two images were used in the test run. The results were compared and confirmed on the pixel by pixel basis for all cloud free land area. The output of the Framework and the offline code were identical when the same compiler was used. This means that the original code we have provided to AIT was correctly reproduced by within the AIT's Framework.

#### 4.2.4.2 Offline Product Validation

The approach to the offline product validation consists in evaluating diurnal variation of the derived GVF. The technique we have implemented uses a dataset of SEVIRI diurnal clear sky observations. This dataset was described in Section 3.4.2 of this document. Diurnal time series were collected for about 880 locations in Europe, Asia and Africa within SEVIRI domain. For every diurnal time series of SEVIRI half-hourly observations, corresponding time series of half-hourly GVF was derived. The daily clear sky GVF data were then used to calculate daily GVF RMSD with equation (3.8). A histogram of RMSD for all pixels was then calculated. To satisfy the precision specifications the GVF diurnal change should not exceed 0.1 for satellite zenith angles below 55 deg and 0.2 for satellite zenith angles within 55 to 70 degrees. GVF diurnal variations exceeding this level are considered excessive. Although a number of external factors may contribute to the excessive diurnal variations in the derived GVF, (undetected clouds, inaccurate navigation, large variation in aerosol concentration, etc.), the principle contribution is supposed to be due to limited accuracy of the NDVI angular anisotropy model. It is expected that GVF product should have less than 20% of cases with excessive diurnal change in GVF at 80% readiness, and less than 10% of cases with excessive GVF diurnal change at 100% readiness. Figure 4.3 shows such comparison of diurnal changes.

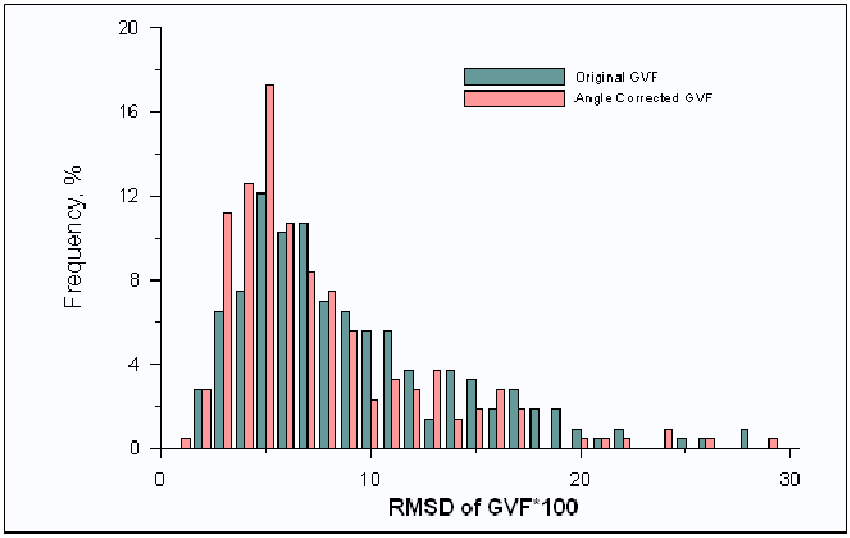


Figure 4.3. Frequency distribution of RMSD in daily GVF retrievals from 880 SEVIRI dataset. Clear sky data have been used. Observations with NDVI < 0.2 were not considered.

In Figure 4.3, the values in green are the results of GVF that is calculated from original observed NDVI. The values in red are the results of GVF that is calculated from corrected NDVI. It is showed that the GVF calculated from corrected NDVI has more cases of small RMSD. Therefore, there is less diurnal change in GVF retrieval calculated from angular corrected NDVI. NDVI angular correction reduces spurious diurnal variations in GVF. However, there is still about 15% of all cases whose diurnal variation in GVF exceeds 0.1. These are mostly observations taken at large (over 55 deg) satellite zenith angle.

Similar approach have been used to calculate SEVIRI full disk clear sky diurnal GVF RMSD for the time period covering days 183 to 245 of years 2008 and 2009. The mean RMSD was equal to 0.066 for all observations taken at satellite zenith angle below 55 degree. For larger satellite zenith angles ranging from 55 to 70 deg, the value of the mean GVF RMSD increased to 0.083.

### 4.2.4.3 Framework Validation

Framework validation technique is the same as the offline technique. AIT members will do 10 week runs of MSG SEVIRI data to generate GVF and other products. The GOES-R ABI Cloud Team's cloud masks will be used to evaluate daily change of GVF for pixels identified as cloud clear for observations made at the same time of the day. The percentage of pixels with excessive (over 0.10/0.2) GVF daily change can then be calculated. It should correspond to those obtained offline with the same test dataset. The results will show here after AIT finish the 10 weeks run.

# 5 PRACTICAL CONSIDERATIONS

## 5.1 Numerical Computation Considerations

The GVF is implemented through simple computation. Some ancillary data flags need to be applied to identify valid land pixels before the computation of GVF. Array computation for the full disk image may require large memory storage. It is recommended to loop through all pixels and compute GVF for pixels that with an valid NDVI value (0.0~1.0), which means that it is a cloud free, snow free, over land pixel, and in good day time condition (i.e., full illumination condition as defined by the product qualifier of < 67° solar zenith angle).

## 5.2 Programming and Procedural Considerations

The GOES-R ABI GVF is a pixel by pixel algorithm, implemented in sequential mode. The model coefficients $C_1$, $C_2$, $NDVI_{max}$ and $NDVI_{min}$ will have to be updated for ABI data. Once these parameters are updated, no routine updates of all model parameter are assumed. However, if there is a new version update just as MODIS products (version 1 through version 5) event, update will be performed.

## 5.3 Quality Assessment and Diagnostics

The quality assessment and diagnostics of GVF should be combined with NDVI since the two products are closely linked. The following procedures are recommended for diagnosing the performance of the NDVI and GVF retrievals.

- Monitor individual NDVI and GVF values periodically. Qualitative analysis of NDVI and GVF spatial distribution and temporal change. These values should be quasi-constant over a large area.
- Abnormally low NDVI and GVF values, lack of spatial uniformity, excessive short-term variations are indicative of cloud contamination.
- Large diurnal changes are due to poor performance of angular anisotropy model.

## 5.4 Exception Handling

All GOES-R algorithms will check the status of the required input data, including primary sensor data, AWG product precedence, and ancillary data. If the input data are of poor quality and could not be used to generate the GOES-R products, quality control (QC) flags will be set and the particular algorithm will exit. The QC flags will be sent back to the framework and the processing will continue to other algorithms.

The GVF algorithm first checks the validity of NDVI from ABI output. If no NDVI or only invalid NDVI presents, the GVF algorithm processing stops. The GVF algorithm also expects the main processing system to flag any pixels where geolocation or viewing geometry information is missing. We emphasize that all pixels that cannot be used to estimate GVF for any reasons, such as clouds, snow, lack of sufficient solar illumination or have invalid measurement data, will be flagged and filled with filling values.

The reason that GVF algorithm does not check for other information is due to the fact that availability of required previously computed GOES-R products such cloud/snow mask and ancillary data such land/sea mask has already been checked in NDVI algorithm. Table 5.1 lists the exception handling needs for NDVI retrievals in the case of missing/bad data. Those QC information in NDVI will directly be ingested into GVF algorithm.

*Table 5.1. Exception handling needs for ABI NDVI algorithm*

| Situation of missing/bad data | What will be generated |
|---|---|
| Pixel is identified as cloudy | "Invalid NDVI" flag in the NDVI file<br>"Cloud" flag in the control file |
| Pixel is over water | "Invalid NDVI" flag in the NDVI file<br>"Water" flag in the control file |
| Insufficient solar illumination (solar zenith angle > 67°) | "Invalid NDVI" flag in the NDVI file<br>"Dark" flag in the control file |
| Derived NDVI value is beyond the [-1.0; 1.0] interval | "Invalid NDVI" flag in the NDVI file<br>"Value outside limits" flag in the control file |
| Corrupted reflectance values (R2 or R3 outside of [0%:100%] range | "Invalid NDVI" flag in the NDVI file<br>"Reflectance value outside limits" flag in the control file |

## 5.5 Algorithm Validation

This section provides a brief overview of pre- and post-launch activities to validate the GOES-R GVF product. A complete description of the GVF validation plan is provided in the “GOES-R GVF Validation Plan” document.

No routine GVF observations are performed on the ground. As a result direct evaluation of the accuracy of GVF estimates is impossible. Consistency of GVF estimates will be assessed indirectly by examining temporal variations in the observed GVF. Large short-term (diurnal and day-to-day) variability in the derived GVF can hardly be due to vegetation cover changes and is typically an indicator of cloud contamination of the time series. Another reason for excessive intraday variation of the derived GVF is inadequate performance of the NDVI angular correction model.

Validation of the GVF product will be conducted on a diurnal change basis by evaluating hourly changes in the derived GVF for each land pixel of the full disk image. For each pixel, every

hourly clear sky GVF data will be used to calculate daily GVF RMSD, and a histogram of RMSD for all pixels will be calculated and compared with precision specifications. The fraction of pixels with the GVF diurnal change over 0.10/0.2 (depending on the location) will be presented as the fraction of invalid GVF retrievals or as the accuracy of the current GVF product.

Validation of the GVF product will also be conducted on a daily basis by evaluating daily changes in the derived GVF for each land pixel of the full disk image. Two hourly images obtained at the same time of the day one day apart will be compared. Pixels identified as clear in both images will be used. The statistics (RMSD) of the difference in estimated GVF in these pairs of pixels will be estimated. The fraction of pixels with the GVF daily difference of over 0.10/0.2 will be presented as the fraction of invalid GVF retrievals or as the accuracy of the current GVF product.

There are two stages in performing the Post-launch validation. At the early stage, which is normally within one to three months after the launch, the algorithm will be be tuned from the results of using the available ancillary datasets. After that, a long-term validation facility and procedure will be performed for assessing and monitoring the GVF product. At that time, algorithm improvement may be available from improving the cloud detection method, the quality of ancillary data, etc.

## 5.6 Other Considerations

Several other considerations are listed below in regard to the current GVF products:

- Instantaneous GVF products have little chance to satisfy the user community. Daily and weekly composite and mostly cloud-free NDVI and GVF products are needed and have to be developed.
- The standard cloud mask may have to be modified or replaced with the mask developed specifically for the GVF product.

The spectral channels used for NDVI estimates in GOES-R ABI are slightly different from corresponding channels in MSG SEVIRI. This may affect both absolute NDVI values as well as the angular anisotropy of NDVI. As a result when the developed algorithm is applied to GOES-R ABI, the GVF model parameters may need adjustment. This concerns both kernel weights in the NDVI angular anisotropy model and the values of minimum and maximum NDVI.

# 6 ASSUMPTIONS AND LIMITATIONS

The following sections describe the current limitations and assumptions in the current version of the GVF.

## 6.1 Assumptions

The following assumptions have been made in developing and estimating the performance of the GVF, including proposed mitigation strategies in parentheses.

- The ABI cloud mask and snow mask are accurate
- NDVI product from ABI is available and is not distorted.

## 6.2 Assumed Sensor Performance

We assume the sensor will meet its current specifications. However, the GVF will be dependent on the following instrumental characteristics.

- Unknown spectral shifts in some channels will cause biases in the performance of the NDVI and hence the GVF.
- Errors in navigation from image to image will affect the performance of the temporal tests or NDVI compositing, and hence the GVF.

## 6.3 Limitations

The following limitations are identified and cautioned for the GVF algorithms and products:

- Possible variations of the atmospheric composition (e.g., aerosol) affect GVF estimates.

## 6.4 Pre-Planned Product Improvements

Plans for GVF product improvements and overcoming identified limitations fall into the following three areas:

- Develop daily and weekly products
  - Less cloud gaps than in the polar product due to high frequency of observations
  - Weekly products are mostly used by climatologists

- Improve angular model
  - Run reflectance and NDVI simulation with 6S and semi-empirical kernel-driven BRDF models
  - Use modeled NDVI to test/improve the developed NDVI angular anisotropy model, and correct kernel weights $C_1$ and $C_2$

- Continue algorithm validation/verification
  - Apply the algorithm to longer observation time series to see the effect of vegetation seasonal change (vegetation phenology)
  - Compare with EUMETSAT Land SAF's Fractional Vegetation Cover (FVC) from MSG/SEVIRI data
  - Compare with NOAA GVF derived from AVHRR data

- Include atmospheric condition in QC
  - 6S or similar code will be used to include AOD (aerosol optical depth) information into the algorithm for QC flag of GVF product
  - Look up tables will be developed to perform operational correction

# 7 REFERENCES


Barlage, M., and X. Zeng (2004). The impact of observed fractional vegetation cover on the land surface climatology in the NCAR climate model. *Journal of Hydrometeorology*, 5:823-830.

Carlson, T. N., and D. A. Ripley (1997). On the relation between NDVI, fractional vegetation cover, and leaf area index, *Remote Sensing of Environment*, 62:241-252.

Ek, M.B., K.E., Mitchell, Y., Lin, E., Rogers, P., Grunmann, V., Koren, G., Gayno and J.D., Tarpley, 2003: Implementation of NOAH land surface model advances in the National Centers for Environmental Prediction operational mesoscale Eta model. *J. Geophys. Res.*, 108, D22, 16pp.

Gallo, K., D. Tarpley, K. Mitchell, I. Csiszar, T. Owen, and B. Reed (2001), Monthly fractional green vegetation cover associated with land cover classes of the conterminous USA, *Geophys. Res. Lett.*, 28(10), 2089–2092, doi:10.1029/2000GL011874.

Gao, F., Y. Jin, X. Li, C. Schaaf, and A. H. Strahler (2002), Bidirectional NDVI and Atmospherically Resistant BRDF Inversion for Vegetation Canopy, *IEEE Trans. Geosci. Remote Sens.*, 40, 1269-1278.

Gutman, G., and A. Ignatov (1998). The derivation of the green vegetation fraction from NOAA/AVHRR data for use in numerical weather prediction models, *International Journal of Remote Sensing*, 19(8):1533-1543.

Hansen, M., R. DeFries, J.R.G. Townshend, and R. Sohlberg (2000), Global land cover classification at 1km resolution using a decision tree classifier, *International Journal of Remote Sensing*. 21:1331-1365.

Hautecoeur, O., and M. M. Leroy (1998), Surface Bidirectional Reflectance Distribution Function observed at global scale by POLDER/ADEOS, *Geophys. Res. Lett.*, 25(22), 4197-4200, 1998GL900111.

Jiang, L., F. N. Kogan, W. Guo, J. D. Tarpley, K. E. Mitchell, M. B. Ek, Y. Tian, W. Zheng, C.-Z. Zou, and B. H.Ramsay (2010), Real-time weekly global green vegetation fraction derived from advanced very high resolution radiometer-based NOAA operational global vegetation index (GVI) system, *J. Geophys. Res.*, 115, D11114, doi:10.1029/2009JD013204.

Leroy, M., J.L. Deuze, F.M. Breon, et al. (1997), Retrieval of atmospheric properties and surface bidirectional reflectances over the land from POLDER/ADEOS, *J. Geophys. Res.*, 102, 17,023-17,037.

LSA SAF Product User Manual (PUM) of Land Surface Analysis Vegetation products (*SAF/LAND/UV/PUM_VEGA/2.1*), February 2008, 53pp.

Lucht, W., C.B. Schaaf, and A.H. Strahler (2000), An Algorithm for the retrieval of albedo from space using semiempirical BRDF models, *IEEE Trans. Geosci. Remote Sens.*, 38, 977-998.

Mitchell, K. E., et al. (2004), The multi-institution North American Land Data Assimilation System (NLDAS): Utilizing multiple GCIP products and partners in a continental distributed hydrological modeling system, *J. Geophys. Res.*, 109, D07S90, doi:10.1029/2003JD003823.

Nilson, T. and A. Kuusk (1989), "A reflectance model for the homogeneous plant canopy and its inversion," *Remote Sens. Environ.*, vol. 27, pp. 157–167.

Roujean, J.-L., M. Leroy, and P. Y. Deschamps (1992), A bidirectional reflectance model of the Earth's surface for the correction of remote sensing data, *J. Geophys. Res.*, vol. 97, pp. 20 455–20 468, 1992.

Schaaf, C. B., F. Gao, A. H. Strahler, W. Lucht, X. Li, T. Tsang, N. C. Strugnell, X. Zhang, Y. Jin, J.-P. Muller, P. Lewis, M. Barnsley, P. Hobson, M. Disney, G. Roberts, M. Dunderdale, C. Doll, R. d'Entremont, B. Hu, S. Liang, and J. L. Privette, and D. P. Roy (2002), First Operational BRDF, Albedo and Nadir Reflectance Products from MODIS, *Remote Sens. Environ.*, 83, 135-148.

Schwartz, M.D., Reed, B.C. and White, M.A. (2002), Assessing satellite-derived start-of-season measures in the conterminous USA, *International Journal of Climatology*, 22, pp. 1793–1805.

Wanner, W., X. Li, and A. H. Strahler (1995), On the derivation of kernels for kernel-driven models of bidirectional reflectance, *J. Geophys. Res.*, vol.100, pp. 21 077–21 090.

Walthall, C. L., J. M. Norman, J. M. Welles, G. Campbell, and B. L. Blad (1985), "Simple equation to approximate the bidirectional reflectance from vegetation canopies and bare soil surfaces," *Appl. Opt.*, vol. 24, pp. 383–387.

Zeng, X., R. E. Dickinson, A. Walker, M. Shaikh, R. S. DeFries, and J. Qi (2000), Derivation and evaluation of global 1-km fractional vegetation cover data for land modeling, *J. Appl. Meteorol.*, 39, 826–839.

Zhou, L., Tucker, C.J., Kaufmann, R.K., Slayback, D., Shabanov, N.V, and Myneni, R.B. (2001), Variations in northern vegetation activity inferred from satellite data of vegetation index during 1981 to 1999, *J. Geophys. Res., 106*, 20069-20083.